Noiseless Quantum Measurement and Squeezing of Microwave Fields Utilizing Mechanical Vibrations

C. F. Ockeloen-Korppi,[1] E. Damskägg,[1] J.-M. Pirkkalainen,[1] T. T. Heikkilä,[2] F. Massel,[2] and M. A. Sillanpää[1,*]
[1]Department of Applied Physics, Aalto University, P.O. Box 15100, FI-00076 AALTO, Finland
[2]Department of Physics and Nanoscience Center, University of Jyväskylä, P.O. Box 35 (YFL) FI-40014 University of Jyväskylä, Finland
(Received 31 October 2016; published 6 March 2017)

A process which strongly amplifies both quadrature amplitudes of an oscillatory signal necessarily adds noise. Alternatively, if the information in one quadrature is lost in phase-sensitive amplification, it is possible to completely reconstruct the other quadrature. Here we demonstrate such a nearly perfect phase-sensitive measurement using a cavity optomechanical scheme, characterized by an extremely small noise less than 0.2 quanta. The device also strongly squeezes microwave radiation by 8 dB below vacuum. A source of bright squeezed microwaves opens up applications in manipulations of quantum systems, and noiseless amplification can be used even at modest cryogenic temperatures.

DOI: 10.1103/PhysRevLett.118.103601

The sensitive measurement of electromagnetic waves is instrumental in science and technology. A sinusoidally oscillating field $X(t) = X_1 \cos(\omega t) + X_2 \sin(\omega t)$ at the frequency ω is characterized by the quadrature amplitudes X_1 and X_2. In quantum mechanics, the quadratures are noncommuting observables which cannot be measured simultaneously. In a usual measurement which responds equally to both quadratures, noise must hence increase by at least half the zero-point fluctuations [1,2].

In a phase-sensitive measurement, the two quadratures are amplified at different gain factors $\mathcal{G}_1$ and $\mathcal{G}_2$, such that the output quadratures are $Y_i = \mathcal{G}_i X_i$. If either of the gains becomes very small and thus the information in this quadrature is discarded, the other quadrature can be perfectly measured. At the same time, the fluctuations in the discarded quadrature can become squeezed below the zero-point fluctuation level. Here we demonstrate such a nearly perfect measurement, proposed very recently [3], of microwave light using a cavity optomechanical setup. Along with the practical device that shows promise for applications, we realize the phase-mixing amplifier [3], and evolve the concept further.

The most sensitive measurements of microwave fields have taken advantage of nonlinearities of Josephson junctions [4–8]. Since late 1980s [9], Josephson junction parametric amplifiers have reached the impressive system noise performance of 0.62 added quanta of noise in the phase-insensitive mode, close to the fundamental limit, and 0.14 quanta in the phase-sensitive mode [10]. Therefore, these amplifiers are currently actively used in quantum science. Also electromechanical systems have been investigated to this end [11–15]. In recent work, Refs. [14,15] demonstrate a phase-insensitive amplifier with a noise relatively low but not quite yet at the quantum limit.

Our realization of a practically noiseless amplifier can be pictured as a generic cavity optomechanical setup. It consists of a superconducting microwave resonator, the cavity, with frequency ω_c, coupled to a 15 μm wide membrane [16] vibrating at the frequency ω_m, as seen in Fig. 1(b). The two systems are coupled via the radiation-pressure coupling $H_{\rm int} = g_0 n_c (b^\dagger + b)$, where $n_c = a^\dagger a$ is the number of microwave cavity photons, $x = b^\dagger + b$ is the (dimensionless) position operator of the mechanical oscillator, and g_0 is a coupling constant. The cavity and the oscillator have the respective decay rates κ and γ. The cavity is driven by two strong microwave tones of frequencies $\omega_+ = \omega_c + \omega_m + \delta$ and $\omega_- = \omega_c - \omega_m - \delta$ [Fig. 1(a)]. The pumps induce respective cavity fields of amplitude α_+ and α_-. Here, δ describes the detuning from the blue or red sideband coresonance condition [17]. The pumping results in an enhanced linear coupling of strength $G_\pm = g_0 \alpha_\pm$.

This pump scheme is related to backaction evading measurements [18] and squeezing [19–21] of the mechanical oscillator, and to the dissipative squeezing recently proposed in Ref. [22]. However, introducing a detuning $\delta \gtrsim (G_-^2 - G_+^2)/\kappa$ drastically changes the resulting physics. In the following, we suppose the resolved-sideband regime, where $\omega_m \gg \kappa$. The Hamiltonian describing this system is [23]

$$H = \delta b^\dagger b + G_+(a^\dagger b^\dagger + ba) + G_-(a^\dagger b + b^\dagger a). \quad (1)$$

We make a Bogoliubov transformation of the cavity to a set of new operators α so that $a = u\alpha - v\alpha^\dagger$. We choose $u = \cosh(\xi)$, $v = \sinh(\xi)$ with the real parameter ξ satisfying $\tanh(\xi) = G_+/G_-$. The resulting cavity-oscillator Hamiltonian is that of a beam splitter with coupling strength $G_{BG} = \sqrt{G_-^2 - G_+^2}$, known to lead to the cooling of the mechanical oscillator [16]. If the cavity is overcoupled, signals sent to it are completely reflected; i.e., the reflected signal at a given frequency ω experiences only a

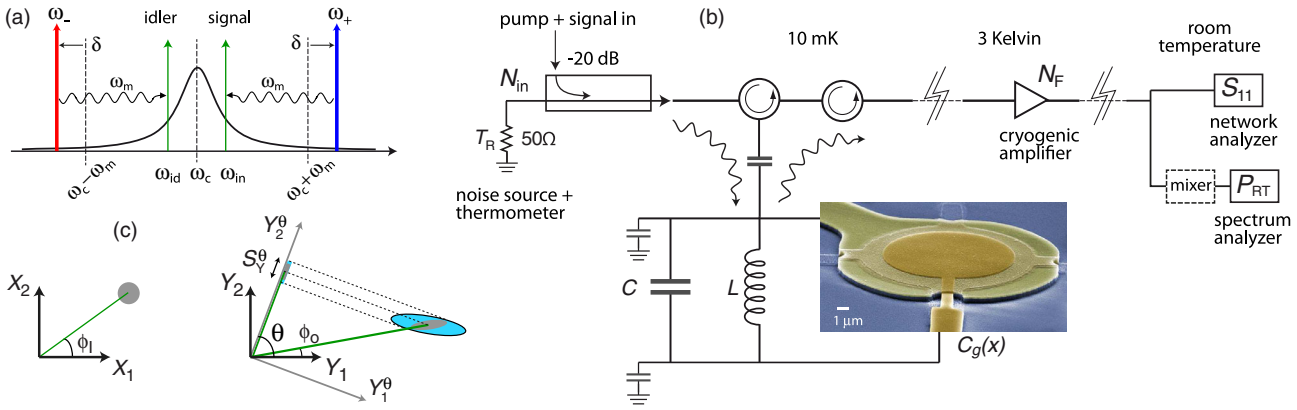

FIG. 1. Optomechanical phase-sensitive measurement. (a) Two strong almost equal-amplitude pump tones (red and blue) are applied detuned from the sideband resonance $\omega_c \pm \omega_m$ by the amount $\delta \lesssim \kappa$. (b) Drumhead-type mechanical oscillator is coupled to a superconducting microwave-frequency (LC) resonator through a radiation-pressure force. A 50 Ω resistor is used as an adjustable noise source with a controlled temperature T_R, directly connected through a directional coupler. The cavity frequency is $\omega_c/2\pi \simeq 6.9148$ GHz, cavity linewidth $\kappa/2\pi \simeq 6.44$ MHz, internal cavity losses $\kappa_I/2\pi \simeq 90$ kHz, frequency of the mechanical mode $\omega_m/2\pi \simeq 10.319$ MHz, and its linewidth $\gamma/2\pi \simeq 107$ Hz. (c) A sinusoidal signal (line) is represented with the quadrature amplitudes X_1 and X_2. Before amplification (left) the gray circle denotes the quantum noise of the input signal. Following phase-sensitive amplification (right) the input quantum noise is squeezed into an ellipse. The total noise at the output has a contribution from the noise added in the process (light blue, ideally none). The signal plus noise is measured in a local oscillator basis defined by the angle θ.

phase shift, or $\alpha_{\rm out}(\omega) = e^{i\phi(\omega)}\alpha_{\rm in}(\omega)$. In a large range of frequencies determining the amplifier bandwidth, different phase shifts of the Bogoliubov wave at positive and negative frequencies translate into phase-sensitive or phase-mixing amplification in the original cavity frame [23]. Even though the mechanical oscillator has a high thermal occupation number $n_m^T \simeq k_b T/\hbar\omega_m \gg 1$, the added noise referred to the input is of the order of $(\gamma\kappa/G_{BG}^2)n_m^T$ and can be almost neglected in our setup. One can thus reach very nearly quantum limited operation even when the mechanical oscillator is far from its quantum ground state.

At this point, let us discuss a phase-sensitive amplifier [1], referring to Fig. 1(c). At the input on top of a coherent signal, there is quantum noise, which usually does not show a phase preference. Hence the possible values of the quadrature amplitudes X_1 and X_2 of the input signal X fall uniformly inside the gray circle representing the variance. Following phase-sensitive amplification, the input noise gets squeezed into an ellipse owing to unequal gains $\mathcal{G}_1$ and $\mathcal{G}_2$ for the input quadratures. The principal axes in the amplified input noise define the preferred (output) quadratures which obey $Y_1 = \mathcal{G}_1 X_1$, $Y_2 = \mathcal{G}_2 X_2$, and the average amplified signal is $Y^2 = 1/2(Y_1^2 + Y_2^2) = \mathcal{G}^2 X^2$, with the total gain $\mathcal{G}$.

Phase-sensitive amplification requires specifying a carrier frequency around which the quadrature operators are defined [1]. In our setup, the carrier frequency is the center frequency of the pumps, $\omega_0 \equiv (\omega_- + \omega_+)/2$ that here also roughly equals ω_c. The carrier frequency not only defines the output quadratures, but the input (preferred) quadratures as well. Therefore, unless the input signal lies exactly at ω_0, a rigorous definition of the input quadratures requires the presence of two fields symmetrically centered around ω_0. The latter case means that one has to consider a field also at the idler (or, image) frequency $\omega_{\rm id}$, satisfying $2\omega_0 = \omega_{\rm in} + \omega_{\rm id}$, as illustrated in Fig. 1(a). In a homodyne detection with a mixer (see below) the information in the idler is retained, which allows for an improved signal compared to phase-insensitive (heterodyne) detection, where the idler is discarded.

A phase-sensitive amplifier can turn into a phase-mixing amplifier when $\omega_{\rm in} \neq \omega_0$ [3]. It differs from the phase-sensitive amplifier because the input-output relations for the quadratures cannot be transformed to the preferred form; i.e., each output quadrature depends through (implicit) gains $\mathcal{G}_{ij}$ on both input quadratures: $Y_1 = \mathcal{G}_{11}X_1 + \mathcal{G}_{12}X_2$ and $Y_2 = \mathcal{G}_{21}X_1 + \mathcal{G}_{22}X_2$. As a result, the ellipse representing the added noise [Fig. 1(c)] is rotated with respect to the input noise ellipse.

A local oscillator (LO) phase θ defines a detection frame for the quadratures. Typically, the detection is in the preferred basis [4,6,10]. In phase-mixing amplifiers, the added noise can have a nontrivial dependence on θ, and the signal-to-noise ratio can potentially be improved by tuning away from the basis defined by the gains. In Fig. 1(c), the detection is indicated by the projections on the Y_2^θ axis. We can hence define a θ dependent gain $\mathcal{G}_\theta$ whose precise form depends on the phase of the input signal. The added noise is referred to the input, that is, the spectral density is $S_X^\theta = S_Y^\theta/\mathcal{G}_\theta^2$, where S_Y^θ represents the output noise when no input signal is present. Expressed in units of quanta at the signal frequency, the phase-dependent added noise is $N_{\rm add}^\theta = S_X^\theta/\hbar\omega_{\rm in}$.

We perform the experiments in a dilution refrigerator. The basic signal scheme is shown in Fig. 1(b). The two

microwave pump tones and a weak signal tone are applied to the coupler port of the device. The amplification is measured with a network analyzer as the S_{11} reflection parameter. In Figs. 2(a)–2(c), we demonstrate phase-insensitive amplification of microwaves achievable with the scheme. The double-peak structure corresponds to the positions of the resonances of the signal and idler, that is, where a phonon in the mechanical oscillator is emitted or absorbed by a pump tone. As shown in Fig. 2(b), we observe high amplification up to 60 dB, or alternatively a broad 3 dB bandwidth ($\simeq$430 kHz). The data shown in Fig. 2(c) correspond to the noise measurements in Fig. 2(d), discussed below. The theoretical predictions [23], overlaid on the experimental data, show a good agreement. In order to quantitatively explain the gain profiles, we include a parametric modulation term to the mechanical oscillator [24]. Notice that in Figs. 2(a)–2(c), we used slightly varying ω_0 (but $\simeq\omega_c$) shifting the peaks.

For noise measurements, we use a 50 Ω resistor as a tunable known noise source. It is attached to a heater and a separate thermometer, and connected to the sample via a short superconducting coaxial cable. At the known calibration temperature T_R, the quantum-noise power from the resistor is $N_{\rm in} = \coth[\hbar\omega_c/(2k_bT_R)]/2$. This calibrated input noise gives rise to an output noise power of $P_{RT} = N_{\rm in}\mathcal{G}^2F + (N_{\rm add} + N_F/\mathcal{G}^2)\mathcal{G}^2F$ at room temperature. Here, F and $N_F \simeq 18 \pm 2$ quanta [23] are, respectively, the gain and the technical noise due to all amplifiers and attenuation following the sample. We use the system noise $N_{\rm eff} \equiv N_{\rm add} + N_F/\mathcal{G}^2$ and $\mathcal{G}^2F$ as adjustable parameters when fitting data to the expression for P_{RT} at varying values of T_R. In Fig. 2(e) we display an example of the measured power, showing a good agreement with the expected quantum noise.

The total (averaged over quadratures) noise corresponds to a phase-insensitive measurement, with the measurement frequency different from ω_0. As shown in Fig. 2(d), we observe a total system noise well below the single quantum level, and the added noise $N_{\rm add}$ is consistent with the quantum limit of 0.5 quanta. The theory curves include dielectric heating of the baths by the pumps up to $n_m^T \simeq 80$, $n_I \simeq 1.1$. Here, n_I is photon occupation of the internal bath of the cavity mode. In a previous cooldown, we made a rough calibration of the bath heating by using sideband cooling, observing a sharp onset of heating around the powers discussed here [23]. The low noise appears clearly

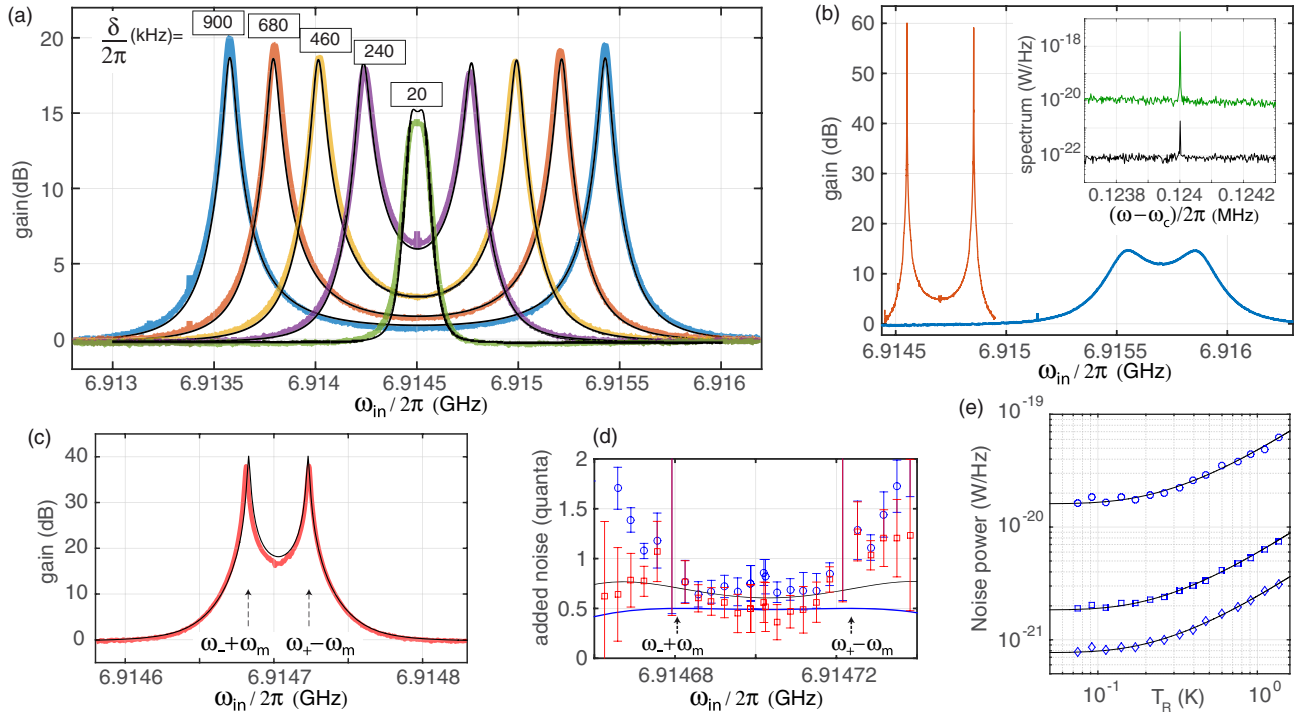

FIG. 2. Phase-insensitive amplification and noise. (a) Gain at a fixed pump power, and at varying pump detunings. Black curves are theory predictions with $G_-/2\pi = 580$ kHz, $G_+/2\pi = 496$ kHz. (b) Amplification at a high gain (red) or over a broad bandwidth (blue). Inset: Improvement of the signal-to-noise ratio of a coherent input signal (sharp peak). The original (black) noise floor is limited by the commercial cryogenic amplifier. When the pump tones are switched on (green) the signal-to-noise ratio in phase-insensitive amplification is improved by 12 dB. (c) Gain for $G_-/2\pi \simeq 308$ kHz, $G_+/2\pi = 304$ kHz, and $\delta/2\pi \simeq 20$ kHz. The black line is a theory prediction. (d) Added noise corresponding to panel (c): Blue circles are the total system noise, and red squares represent the added noise due to the optomechanical amplification. The solid black line is a theory curve, while the blue line shows the quantum limit [25]. (e) Noise calibration by varying the power emitted by a known noise source. The noise at device output is shown. The data sets correspond to $\omega_{\rm in}/2\pi = 6.914\,682$, $6.914\,686$, and $6.914\,689$ GHz, in (c) from top to bottom. The solid lines are fits to the quantum-noise formula.

as an improvement of signal-to-noise ratio of a weak signal when the amplification is switched on, as displayed in Fig. 2(b) (inset) where the observed noise floor is dominated by amplified vacuum noise. Figure 2(d) shows that the added noise can be very close to 0.5 quanta even when the mechanical oscillator responsible for the amplification resides far from its ground state.

For phase-sensitive homodyne measurements, the output signal is digitally mixed to the center frequency $\omega_{\mathrm{LO}} = \omega_0$ in the scheme of Fig. 3(a). By changing the phase θ of the LO, we obtain the quadratures $Y_1^\theta(t)$ and $Y_2^\theta(t) = Y_1^{\theta+\pi/2}(t)$ oscillating at the center frequency. The noise measurements are made as described above, but individually for each θ [23]. We discover that the noise falls well below the quantum limit in one quadrature [Fig. 3(b)] and we estimate $N_{\mathrm{add}} \lesssim 0.2$ quanta. The uncertainty is dominated by the statistical errors from fitting to the quantum noise. The theoretical added noise [3,23] (black) in Fig. 3(b) is evaluated using $n_m^T \simeq 300$, $n_I \simeq 1.5$, capturing the main features involving the optimum noise offset from the preferred quadrature.

A fundamental property of a phase-sensitive amplifier is the possibility to generate squeezed propagating states as shown in many experiments in optics [26,27], and with Josephson devices, see, e.g., [6,9]. Quantum squeezing of the light emitted from optomechanical cavities has also recently been observed at optical frequencies [28–30]. Next, we show that our approach provides a way to generate squeezed radiation. This demonstrates a new mechanism over the previously utilized ponderomotive squeezing [28–30]. In the plane of the input of the cryogenic amplifier, we measure strong squeezing within a bandwidth of 700 kHz, with the maximum of ≃3.5 dB below vacuum, as shown in Fig. 4. The calibration procedure is described in the Supplemental Material [23]. The theory predictions in Figs. 4(b)–4(d) are generated using $n_m^T = 400$, $n_I = 1.6$. We infer that the amount of squeezing, depleted by losses before the cryogenic amplifier, right following the sample has been up to 8 dB. This value is on par with those obtained with Josephson parametric amplifiers (JPA), e.g., 10 dB in Ref. [6].

Intense squeezed coherent states are a valuable resource [31–34]. When injected with a sinusoidal signal, we estimate the setup of Fig. 4 to produce a bright squeezed coherent state of up to $\sim 10^{14}$ photons/sec, or ~ -65 dBm. If realized in optics, our approach can provide luminous squeezed laser beams to overcome the quantum-noise limitation in gravitational wave observations. Our amplification scheme compares favorably over JPA because it does not require superconductivity, and is able to handle 4 orders of magnitude more input power than a corresponding JPA [6], or 2 orders of magnitude more than in Ref. [8]. Moreover, in contrast to cavity-based parametric amplifiers, the gain-bandwidth product is unlimited [23]. The bandwidth is smaller than in JPA, but it can be increased by stronger coupling, or by implementing an electromechanical metamaterial. With slight improvements, the device can operate below the

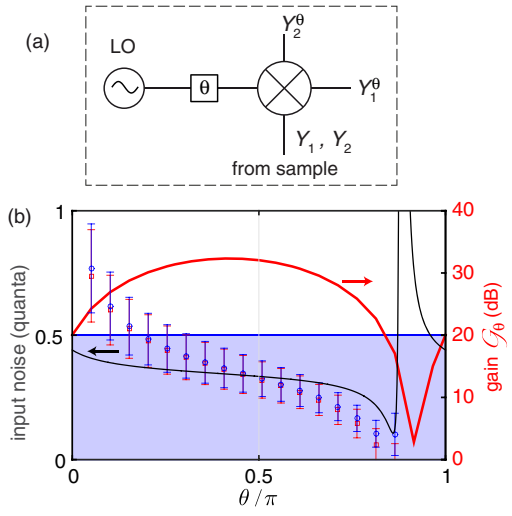

FIG. 3. Phase-mixing amplification. (a) In homodyne detection, a mixer [dashed box in Fig. 1(b)] extracts the quadrature amplitudes oscillating at the local oscillator (LO) frequency ω_{LO}. The quadrature axes Y_1^θ and Y_2^θ are determined by the digitally tunable phase shift θ. (b) Input noise (left scale) and gain (right scale) as a function of quadrature angle θ. The blue circles are the system noise N_{eff}^θ, and the red squares the added noise N_{add}^θ. The black curve is the prediction for N_{add}^θ. The regime below the quantum limit is colored in blue. The parameters are $G_-/2\pi \simeq 320$ kHz, $G_+/2\pi \simeq 315$ kHz, $\delta/2\pi \simeq 460$ kHz, and $\omega_{\mathrm{in}}/2\pi = 6.915\,165$ GHz.

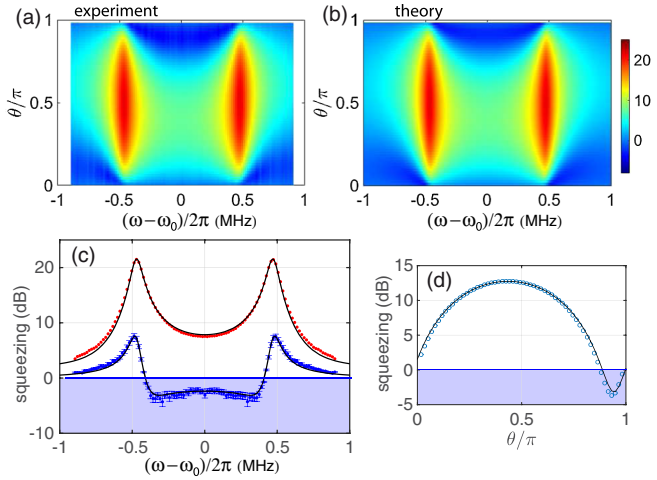

FIG. 4. Mechanical squeezing of microwave light. (a) Noise emitted from the device normalized to the vacuum level (in dB) as a function of the local oscillator phase θ and frequency. (b) Theoretical prediction corresponding to (a). (c) Crosscut along the horizontal lines $\theta \simeq 2.93$ (blue) and $\theta = 1.38$ (red). The thin solid lines are the corresponding theoretical curves. (d) Squeezing at $\omega/2\pi = -0.369$ MHz as a function of θ. In (c) and (d) the area under the zero-point fluctuation level is colored in blue. The pump amplitudes are $G_-/2\pi \simeq 690$ kHz, $G_+/2\pi \simeq 590$ kHz.

quantum limit at modest cryogenic temperatures of a few kelvin, hence offering an attractive technology for narrow-band measurements in particle physics [35], with superconducting qubits [36–38], or finally, in microwave optomechanics.

We thank Visa Vesterinen, Pasi Lähteenmäki, and Timo Hyart for useful discussions. This work was supported by the Academy of Finland (Contracts No. 250280, No. CoE LTQ, No. 275245), by the European Research Council (No. 240387-NEMSQED, No. 240362-Heattronics, No. 615755-CAVITYQPD), the Horizon 2020 programme (No. FETPROACT-2016 732894-HOT), and the Centre for Quantum Engineering at Aalto University. The work benefited from the facilities at the OtaNano–Micronova Nanofabrication Center and at the Low Temperature Laboratory.

*mika.sillanpaa@aalto.fi

[1] C. M. Caves, Phys. Rev. D **26**, 1817 (1982).
[2] A. A. Clerk, M. H. Devoret, S. M. Girvin, F. Marquardt, and R. J. Schoelkopf, Rev. Mod. Phys. **82**, 1155 (2010).
[3] C. F. Ockeloen-Korppi, T. T. Heikkilä, M. A. Sillanpää, and F. Massel, arXiv:1610.07579.
[4] B. Yurke, P. G. Kaminsky, R. E. Miller, E. A. Whittaker, A. D. Smith, A. H. Silver, and R. W. Simon, Phys. Rev. Lett. **60**, 764 (1988).
[5] N. Bergeal, F. Schackert, M. Metcalfe, R. Vijay, V. E. Manucharyan, L. Frunzio, D. E. Prober, R. J. Schoelkopf, S. M. Girvin, and M. H. Devoret, Nature (London) **465**, 64 (2010).
[6] M. A. Castellanos-Beltran, K. D. Irwin, G. C. Hilton, L. R. Vale, and K. W. Lehnert, Nat. Phys. **4**, 929 (2008).
[7] C. Eichler, Y. Salathe, J. Mlynek, S. Schmidt, and A. Wallraff, Phys. Rev. Lett. **113**, 110502 (2014).
[8] C. Macklin, K. O'Brien, D. Hover, M. E. Schwartz, V. Bolkhovsky, X. Zhang, W. D. Oliver, and I. Siddiqi, Science **350**, 307 (2015).
[9] R. Movshovich, B. Yurke, P. G. Kaminsky, A. D. Smith, A. H. Silver, R. W. Simon, and M. V. Schneider, Phys. Rev. Lett. **65**, 1419 (1990).
[10] L. Zhong, E. P. Menzel, R. D. Candia, P. Eder, M. Ihmig, A. Baust, M. Haeberlein, E. Hoffmann, K. Inomata, T. Yamamoto, Y. Nakamura, E. Solano, F. Deppe, A. Marx, and R. Gross, New J. Phys. **15**, 125013 (2013).
[11] F. Massel, T. T. Heikkilä, J.-M. Pirkkalainen, S. U. Cho, H. Saloniemi, P. J. Hakonen, and M. A. Sillanpää, Nature (London) **480**, 351 (2011).
[12] T. G. McRae and W. P. Bowen, Appl. Phys. Lett. **100**, 201101 (2012).
[13] T. Bagci, A. Simonsen, S. Schmid, L. G. Villanueva, E. Zeuthen, J. Appel, J. M. Taylor, A. Sørensen, K. Usami, A. Schliesser, and E. S. Polzik, Nature (London) **507**, 81 (2014).
[14] C. F. Ockeloen-Korppi, E. Damskägg, J.-M. Pirkkalainen, T. T. Heikkilä, F. Massel, and M. A. Sillanpää, Phys. Rev. X **6**, 041024 (2016).
[15] L. D. Tóth, N. R. Bernier, A. Nunnenkamp, E. Glushkov, A. K. Feofanov, and T. J. Kippenberg, arXiv:1602.05180.
[16] J. D. Teufel, D. Li, M. S. Allman, K. Cicak, A. J. Sirois, J. D. Whittaker, and R. W. Simmonds, Nature (London) **471**, 204 (2011).
[17] Notice that generally the pumps need not be symmetrically detuned with respect to ω_c. For simplicity, we focus on the (optimum) case of symmetric detuning.
[18] J. Suh, A. J. Weinstein, C. U. Lei, E. E. Wollman, S. K. Steinke, P. Meystre, A. A. Clerk, and K. C. Schwab, Science **344**, 1262 (2014).
[19] E. E. Wollman, C. U. Lei, A. J. Weinstein, J. Suh, A. Kronwald, F. Marquardt, A. A. Clerk, and K. C. Schwab, Science **349**, 952 (2015).
[20] J.-M. Pirkkalainen, E. Damskägg, M. Brandt, F. Massel, and M. A. Sillanpää, Phys. Rev. Lett. **115**, 243601 (2015).
[21] F. Lecocq, J. B. Clark, R. W. Simmonds, J. Aumentado, and J. D. Teufel, Phys. Rev. X **5**, 041037 (2015).
[22] A. Kronwald, F. Marquardt, and A. A. Clerk, New J. Phys. **16**, 063058 (2014).
[23] See Supplemental Material at http://link.aps.org/supplemental/10.1103/PhysRevLett.118.103601 for experimental and theoretical details.
[24] J. Suh, M. D. Shaw, H. G. LeDuc, A. J. Weinstein, and K. C. Schwab, Nano Lett. **12**, 6260 (2012).
[25] The quantum limit of added noise is below 0.5 if the gain is not very large.
[26] R. E. Slusher, L. W. Hollberg, B. Yurke, J. C. Mertz, and J. F. Valley, Phys. Rev. Lett. **55**, 2409 (1985).
[27] L.-A. Wu, H. J. Kimble, J. L. Hall, and H. Wu, Phys. Rev. Lett. **57**, 2520 (1986).
[28] D. W. C. Brooks, T. Botter, S. Schreppler, T. P. Purdy, N. Brahms, and D. M. Stamper-Kurn, Nature (London) **488**, 476 (2012).
[29] A. H. Safavi-Naeini, S. Groblacher, J. T. Hill, J. Chan, M. Aspelmeyer, and O. Painter, Nature (London) **500**, 185 (2013).
[30] T. P. Purdy, P.-L. Yu, R. W. Peterson, N. S. Kampel, and C. A. Regal, Phys. Rev. X **3**, 031012 (2013).
[31] A. Furusawa, J. L. Sørensen, S. L. Braunstein, C. A. Fuchs, H. J. Kimble, and E. S. Polzik, Science **282**, 706 (1998).
[32] K. Jähne, C. Genes, K. Hammerer, M. Wallquist, E. S. Polzik, and P. Zoller, Phys. Rev. A **79**, 063819 (2009).
[33] K. W. Murch, S. J. Weber, K. M. Beck, E. Ginossar, and I. Siddiqi, Nature (London) **499**, 62 (2013).
[34] J. B. Clark, F. Lecocq, R. W. Simmonds, J. Aumentado, and J. D. Teufel, Nat. Phys. **12**, 683 (2016).
[35] S. J. Asztalos, G. Carosi, C. Hagmann, D. Kinion, K. van Bibber, M. Hotz, L. J. Rosenberg, G. Rybka, J. Hoskins, J. Hwang, P. Sikivie, D. B. Tanner, R. Bradley, and J. Clarke, Phys. Rev. Lett. **104**, 041301 (2010).
[36] R. Vijay, D. H. Slichter, and I. Siddiqi, Phys. Rev. Lett. **106**, 110502 (2011).
[37] D. Ristè, J. G. van Leeuwen, H.-S. Ku, K. W. Lehnert, and L. DiCarlo, Phys. Rev. Lett. **109**, 050507 (2012).
[38] N. Ofek, A. Petrenko, R. Heeres, P. Reinhold, Z. Leghtas, B. Vlastakis, Y. Liu, L. Frunzio, S. M. Girvin, L. Jiang, M. Mirrahimi, M. H. Devoret, and R. J. Schoelkopf, Nature (London) **536**, 441 (2016).